Diagram technique for a 2D system of interacting electrons in a strong magnetic field

A. V. Andreev and Yu. A. Bychkov

L. D. Landau Institute of Theoretical Physics, Academy of Sciences of the USSR
(Submitted 19 March 1991)
Zh. Eksp. Teor. Fiz. **100**, 725–733 (August 1991)

Certain features of the diagram technique for a polarized 2D system of interacting particles in a magnetic field are analyzed. It is assumed that the interaction does not cause electron transitions from one Landau level to another. In a given order of perturbation theory, topologically different diagrams fall into groups within which all diagrams are equal. A principle governing the combining of equivalent diagrams is formulated. The number of such diagrams is found. A class of diagrams equivalent to an electron-hole interaction is identified. The summation of these diagrams leads to a singularity in the scattering amplitude, which is in turn responsible for an instability with respect to the excitation of charge density waves.

1. INTRODUCTION

A two-dimensional (2D) system in a magnetic field **B** perpendicular to the plane of motion of the particles has an exceedingly important property: The energy of the particles depends only on the index of the Landau level and is degenerate in terms of the position of the center of the orbit (in the Landau gauge). This degeneracy leads to major difficulties in efforts to study the interaction between particles in such a system. The first attempt to determine the nature of the interaction of electrons in a 2D system in a strong magnetic field was undertaken in Ref. 1. The problem attracted a flurry of interest after the discovery of the fractional quantum Hall effect and the very important paper by Laughlin which followed.[2] Among the extremely long list of papers which have been devoted to this problem, the studies by Lerner and Lozovik stand out (see Ref. 3 and the bibliography there). Those authors were apparently the first to use quantum field-theory methods to solve the problem. In the model which they used, they succeeded to a large extent in overcoming the difficulties stemming from the degeneracy of the seed spectrum of particles for the case of a neutral 2D system.

In the present paper we continue the study of the general properties of a diagram technique for a 2D system in a strong magnetic field which was begun by one of the present authors in Ref. 4. The model we will be using is based on the widely accepted condition that the Coulomb energy of the particles, $\varepsilon_c = e^2/\varkappa l_B$ [$\varkappa$ is the dielectric constant, and $l_B = (c\hbar/eB)^{1/2}$ is the magnetic length] is much smaller than the distance between Landau levels; i.e., the interaction conserves the number of particles in a given Landau level. The system is assumed to be polarized, so we will be omitting the spin indices.

The analysis below shows that in a given order of perturbation theory all the diagrams fall into certain groups of topologically different diagrams. Within each group, the diagrams are equal. We formulate a general principle for determining a class of equivalent diagrams and for finding their number. We show that a summation of diagrams which are equivalent to the incorporation of polarization loops (which in turn corresponds to a summation of "zero-sound" loops) leads to a singularity in the scattering amplitude. This singularity is associated with an instability with respect to the formation of charge density waves.[5]

2. INTERACTION HAMILTONIAN AND ITS PROPERTIES

In the Landau gauge with the vector potential $\mathbf{A} = (0, Bx, 0)$, the wave function of a particle in a magnetic field **B** is

$$\psi_n(\rho) = L^{-1/2} e^{iky} \varphi_n(x-k), \tag{1}$$

where distances are expressed in units of l_B, L is the size of the system, $\varphi_n(x)$ is a normalized simple-harmonic-oscillator wave function, and n is the index of the Landau level. Using (1), we can write the interaction Hamiltonian of the system as[6]

$$\hat{H}_{int} = \frac{1}{2} \sum_{k_1,k_2} \int \frac{d\mathbf{q}}{(2\pi)^2} \tilde{V}_n(q)$$
$$\times \exp[iq_x(k_1-k_2-q_y)] \hat{a}_{k_1}^+ \hat{a}_{k_2}^+ \hat{a}_{k_2'} \hat{a}_{k_1'},$$
$$\tilde{V}_n(q) = V(q) w_n^2(q^2), \quad k_1' = k_1 - q_y, \quad k_2' = k_2 + q_y, \tag{2}$$

where the operator $\hat{a}_k$ ($\hat{a}_k^+$) annihilates (creates) a particle with a momentum k. Here $V(q)$ is the Fourier component of the interaction potential,

$$w_n(x) = e^{-x/4} L_n(x/2),$$

and $L_n(x)$ is the Laguerre polynomial.

The Hamiltonian (2) allows a very important transformation. We first write the obvious identity

$$\tilde{V}_n(q) \equiv \int \delta(\mathbf{q}-\mathbf{p}) \tilde{V}_n(p) d\mathbf{p} = \frac{1}{2\pi} \int e^{-i\mathbf{q}\mathbf{l}} \tilde{V}_n'(l) dl, \tag{3}$$

where

$$\tilde{V}_n'(q) = \frac{1}{2\pi} \int \tilde{V}_n(p) e^{i\mathbf{p}\mathbf{q}} d\mathbf{p} \tag{4}$$

is a new effective potential. This identity makes it possible to identify the dependence on the momentum **q** explicitly. Substituting the last expression in (3) for $\tilde{V}_n(q)$ into the Hamiltonian (2), we can carry out the integration over the variable q_x (which is not included among the indices of the particle creation and annihilation operators). After some very simple transformations and changes in notation, our initial Hamiltonian (2) becomes

$$\hat{H}_{int} = \frac{1}{2} \sum_{k_1,k_2} \int \frac{d\mathbf{q}}{(2\pi)^2} \tilde{V}_n'(q)$$
$$\times \exp[iq_x(k_1-k_2-q_y)] \hat{a}_{k_1}^+ \hat{a}_{k_2}^+ \hat{a}_{k_1'} \hat{a}_{k_2'}. \tag{5}$$

The transformations which have been carried out have changed the potential and have interchanged the indices on the particle annihilation operators. Taking half the sum of expressions (2) and (5), we find that the effective interaction potential is determined by the potential

$$\tilde{U}_n(q) = {}^1\!/_2[\tilde{V}_n(q) - \tilde{V}_n{}'(q)],\tag{6}$$

Using the definition (4), we see that the following condition holds:

$$\tilde{U}_n(q) = -\frac{1}{2\pi}\int e^{iqp}U_n(p)dp.\tag{7}$$

The physical meaning of the potential $\tilde{U}_n(p)$ is extremely simple.[4] Examining a two-particle problem,[1] we easily see that the only energy levels which enter the potential (6) are those which correspond to an antisymmetric function of two electrons.

The effective Hamiltonian is therefore

$$\hat{H}_{int} = \frac{1}{2}\sum_{k_1,k_2}\int\frac{d\mathbf{q}}{(2\pi)^2}\tilde{U}_n(q)$$

$$\times \exp[iq_x(k_1-k_2-q_y)]\hat{a}_{k_1}{}^+\hat{a}_{k_2}{}^+\hat{a}_{k_2'}\hat{a}_{k_1'}\tag{8}$$

and relation (7) holds. As a result of that relation, we can interchange the indices on the annihilation operators in (8) without interchanging the operators themselves; in the process we of course change the sign of the expression. A subsequent interchange of the annihilation operators restores the sign of the Hamiltonian. We turn now to some consequences of this symmetry of the Hamiltonian (8).

3. PROPERTIES OF DIAGRAMS FOR A TWO-PARTICLE GREEN'S FUNCTION

In this section of the paper we make use of the well-known diagram-technique methods from the theory of interacting particles.[7] We wish to stress that the temperature technique must be used because the system is degenerate in the absence of an interaction.

The most important quantities are the one-particle and two-particle Green's functions

$$G_{p,\,p'}(\tau,\,\tau') = -\langle T_\tau(\hat{a}_p(\tau)\hat{a}_{p'}{}^+(\tau'))\rangle,\tag{9}$$

$$G^{(2)}_{p_1p_2,p_1'p_2'}(\tau_1,\tau_2;\tau_1',\tau_2')$$

$$= \langle T_\tau(\hat{a}_{p_1}(\tau_1)\hat{a}_{p_2}(\tau_2)\hat{a}_{p_2'}^+(\tau_2')\hat{a}_{p_1'}^+(\tau_1'))\rangle.\tag{10}$$

The angle brackets denote a thermodynamic average, and T_τ indicates the "chronological" ordering.

The most interesting results which follow from the properties of Hamiltonian (8) can be seen through a study of the diagrams beginning in second-order perturbation theory for the function (10). Corresponding diagrams are shown in Fig. 1. We first use the example of diagram b in Fig. 1 to explain the method for constructing the corresponding analytic expression. For this diagram the corresponding analytic expression is

$$\sum_{\substack{\mathbf{q},\mathbf{q}',\\k_1,k_2;l_1,l_2}}\tilde{U}_n(q)\tilde{U}_n(q')\exp[iq_x(k_1-k_2-q_y)+iq_x'(l_1-l_2-q_y')]$$

$$\times G_{p_1k_1}G_{k_1'l_1}G_{l_1'k_2}G_{k_2'p_1'}G_{p_2l_2}G_{l_2'p_2'}.\tag{11}$$

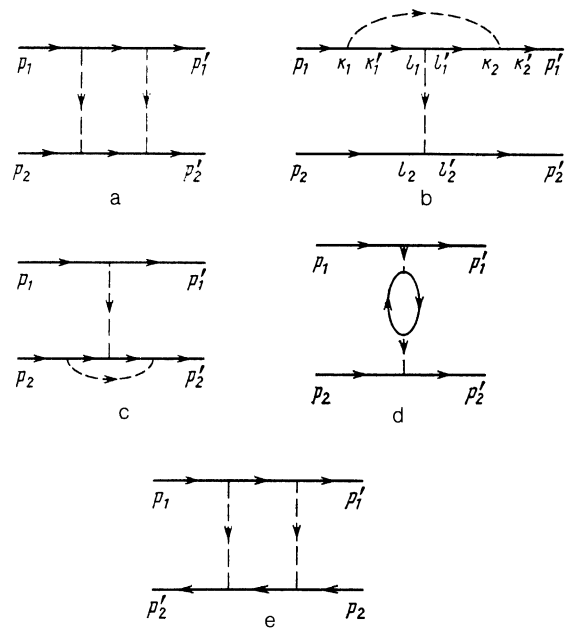The general scheme for constructing the corresponding

FIG. 1. Diagrams of second-order perturbation theory for two-particle Green's function (10). In addition to the diagrams shown here, there are five more like diagrams a–e, which differ from the ones shown by an interchange of the momenta p_1', p_2' and a change in sign. All the momenta are specified for diagram b.

expression for an arbitrary diagram is as follows. With each line we associate a one-particle Green's function with the initial and final momenta (in the direction of the arrow). With each dashed line we associate a potential $\tilde{U}_n(q)$ and a factor $\exp[iq_x(k_1-k_2-q_y)]$. The momentum k_1 corresponds to the base of a dashed line (which specifies the direction), and k_2 corresponds to a vertex. From conservation of the y component of the momentum we have the conditions $k_1' = k_1 - q_y, k_2' = k_2 + q_y$. A summation must be carried out over all the internal variables.

As we established above, the transformation (7) alters the sign of the potential and interchanges the corresponding momenta ($k_1' \leftrightarrow k_2'$) for a given $\tilde{U}_n(q)$. For the case of diagram b in Fig. 1, this transformation can be carried out either in terms of each variable $\mathbf{q}$, $\mathbf{q}'$ independently or in terms of the two variables simultaneously. A transformation of expression (11) in terms of the variable $\mathbf{q}$ leads to a new sequence of indices in the Green's function. The corresponding part of expression (11) becomes

$$G_{p_1k_1}G_{k_1'p_1'}G_{p_2l_2}G_{l_2'p_2'}G_{l_1'k_2}G_{k_2'l_1}.\tag{12}$$

This arrangement of Green's functions, however, corresponds to diagram d in Fig. 1; taking the signs into account, we can say that diagrams b and d are equal. Carrying out a transformation in terms of the momentum $\mathbf{q}'$ alone, and then carrying out the corresponding transformation in terms of $\mathbf{q}$ and $\mathbf{q}'$ simultaneously, we find that diagrams b, c, d, and e' (see the Fig. 1 caption) are equal.

It is completely clear that for an arbitrary diagram of mth order the total number of all possible transformations is

$$\sum_{k=1}^{m}C_m{}^k = 2^m - 1,$$

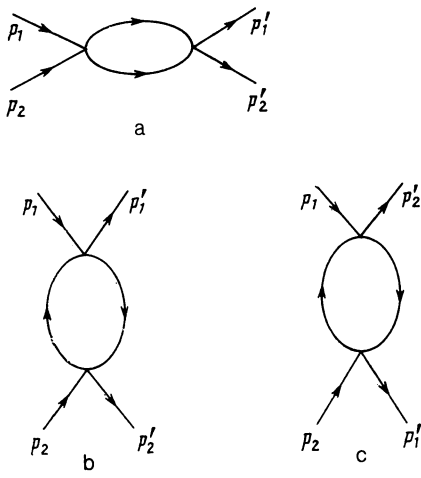where the $C_m{}^k$ are the binomial coefficients. We cannot in

A. V. Andreev and Yu. A. Bychkov   405

FIG. 2. Skeletal diagrams obtained from Fig. 1 by reducing the dashed lines to a single point.

FIG. 3. Skeletal diagrams in third-order perturbation theory. Diagrams which differ from those shown by an interchange of the final momenta p_1', p_2' are not shown.

general assert that all these transformations lead to topologically different diagrams. In particular, the simple example of diagram a shows that its topological structure does not change at all in the course of any of the transformations (however, some of the transformations do change the positions of the momenta p_1' and p_2').

To explain the result obtained in second-order perturbation theory, we redraw the diagrams in Fig. 1 in a slightly different way. We introduce "skeletal" diagrams, reducing the corresponding vertex (containing the given dashed line) to a point. As a result we find the skeletal diagrams in Fig. 2. There is a very important point to note here: All the diagrams which go into each other under transformation (7), i.e., which are equivalent, correspond to the same skeletal diagram. If we now wish to go back from diagram b in Fig. 2 to find the corresponding diagrams in Fig. 1, the rule is obvious: The number of ways in which we can do this is 4 (2^m, where m is the order of the perturbation theory), since there are two ways to insert a dashed line in each vertex. A very important difference between diagrams a and b is that the loop in diagram b is a "zero-sound" loop, by which we mean that the electron lines in it are oppositely directed.

Figure 3 shows the skeletal diagrams of third-order perturbation theory. Corresponding to diagram a there is only one diagram, which is analogous to diagram a in Fig. 1. Four topologically different diagrams correspond to each of diagrams b and c. Diagrams d–f are equivalent to 8 (2^m, $m = 3$) different diagrams. Diagrams g and h contain a "Cooper" loop, by which we mean a loop in which the electron lines are parallel. Each is equivalent to 4 (2^{m-1}, $m = 3$) different diagrams. As an example, we show in Fig. 4A diagrams which are equal to each other and equivalent to skeletal diagram d in Fig. 3, while in Fig. 4B we show diagrams which are equivalent to the skeletal diagram g in Fig. 3. Here it is particularly obvious that diagrams which are completely different in topological structure are equal to each other. In particular, diagrams which contain polarization loops and those which do not are equivalent.

We can now put the rule for finding the number of equivalent diagrams in a given order of perturbation theory in its final form. First, we have to find all the different skeletal diagrams. Diagrams which belong to different skeletal
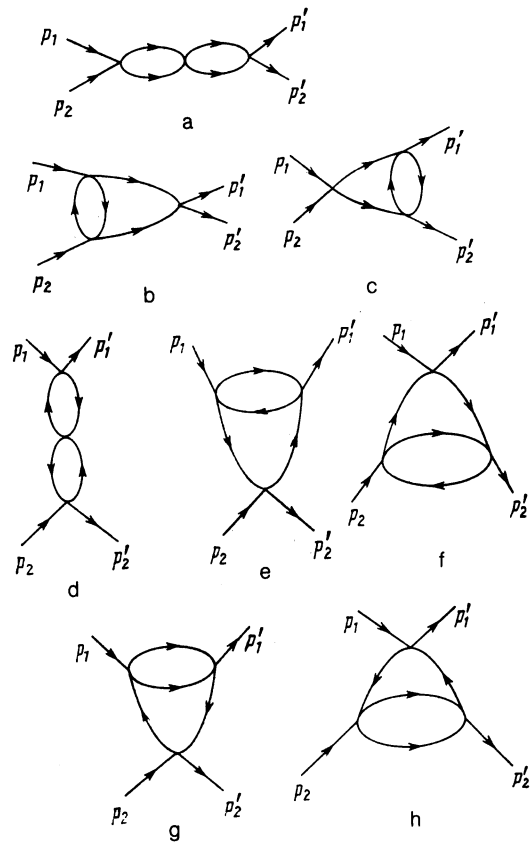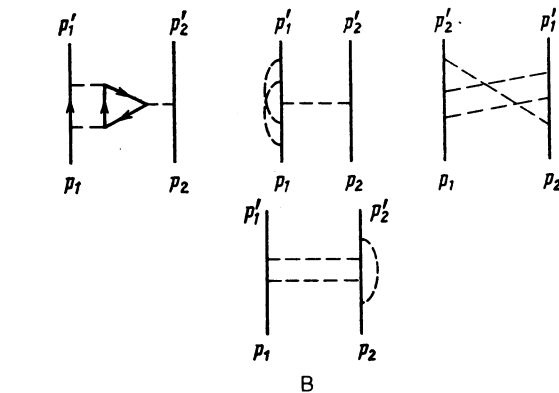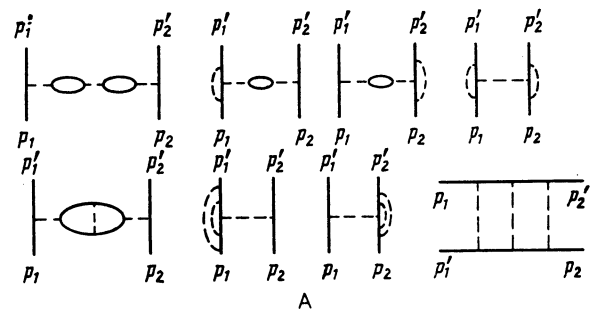

FIG. 4. A—Diagrams which are equivalent to skeletal diagram d in Fig. 3; B—diagrams which are equivalent to diagram g in Fig. 3.

diagrams are not equivalent. For a given skeletal diagram the number of equivalent diagrams is 2^{m-k}, where m is the order of the perturbation theory, and k is the number of Cooper loops. This rule applies to diagrams which are not reducible in terms of initial and final momenta, i.e., diagrams which cannot be cut along two parallel lines and thereby broken up into two parts, which contain only incoming momenta (p_1,p_2) and only outgoing momenta (p_1',p_2'). Diagrams a–c in Fig. 3 are examples of reducible diagrams of this type. The number of reducible equivalent diagrams is determined by the number of nontrivial irreducible insertions.

4. ANALYSIS OF THE DIAGRAMS

As we know, diagrams of the type in Fig. 3 are "parquet" diagrams.[8] Beginning in fourth-order perturbation theory, we find diagrams which are structurally more complex. However, there is also definite interest in analyzing simple loops, one of which is a Cooper loop which describes the scattering of two electrons against the background of the other particles. A loop of this sort is shown in Fig. 2a. According to the well-known rules,[7] the contribution of this diagram is proportional to the sum

$$T \sum_\omega G_0(\omega) G_0(\omega_1 + \omega_2 - \omega), \qquad (13)$$

where

$$G_0(\omega) = \frac{1}{i\omega - \xi},$$

$\omega = \pi T(2n + 1)$, ξ is the energy of the particle, reckoned from the chemical potential, and $\omega_{1,2}$ are the frequencies of incoming lines. Elementary calculations put expression (13) in the final form

$$\frac{1}{i(\omega_1 + \omega_2) - 2\xi}(2f - 1), \qquad (14)$$

where $f(\xi) = [1 + \exp(\xi/T)]^{-1}$ is a Fermi distribution function. On the other hand, $f = \nu = 2\pi l_B^2 n_s$ is the dimensionless degree of filling of the Landau level (n_s is the density of electrons). It follows that for $\nu = \frac{1}{2}$ the scattering of electrons by one another can be significantly suppressed. Another interesting fact is that with $\nu = \frac{1}{2}$ there is no singularity of the form (14) in terms of the sum frequency $\omega_1 + \omega_2$ and ξ even for the very simple "envelope" diagram (see Ref. 8 for definitions of parquet diagrams and more-complex diagrams).

We turn now to diagram b in Fig. 2. We recall that it describes some very different processes which correspond to diagrams b–e in Fig. 1. The latter diagrams correspond to both scattering of an electron by a hole and renormalization of the interaction potential for the polarization loop. The contribution of this loop is proportional to the sum

$$T \sum_\omega G_0(\omega) G_0(\omega + \omega_1 - \omega_1') = \delta_{\omega_1,\omega_1'} \frac{\partial f}{\partial \xi} = -\delta_{\omega_1,\omega_1'} \frac{\nu(1-\nu)}{T}. \qquad (15)$$

This result is a consequence of the degeneracy of the spectrum of particles. A summation of all such loops leads to the following renormalized interaction potential:

$$\int \frac{dq_x}{\pi} \exp[iq_x(p_1 - p_2')] U_n(q) \left[1 - \frac{1}{\pi} U_n(q) \frac{\partial f}{\partial \xi}\right]^{-1}, \qquad (16)$$

$$\mathbf{q} = (q_x, p_1 - p_1').$$

An explicit expression for the denominator of the expression in (16) [see (6)] is

$$1 - \frac{\nu(1-\nu)}{T} \frac{1}{2\pi} \left[\frac{1}{2\pi} \int e^{i\mathbf{qp}} \tilde{V}_n(p) d\mathbf{p} - \tilde{V}_n(q)\right], \qquad (17)$$

where $\mathbf{q} = (q_x, p_1 - p_1')$.

As the temperature is lowered, expression (17) may vanish; beginning at a certain temperature, it may vanish over an entire interval of the momentum $\mathbf{q}$. This is a very important result. It is directly related to the instability with respect to the excitation of charge density waves, which was observed in Ref. 5 but which was found there on the basis of entirely different considerations. We regard this result as unexpected. The reason is that the series which was summed is equivalent to the incorporation of polarization loops, which usually leads to screening of the potential. Instead of screening in this case we find instability against excitation of charge density waves. In other words, expression (16) represents the amplitude for the scattering of an electron by a hole. The contributions of the Cooper loops in (14) and the electron-hole interaction in (15) are in general comparable in magnitude (each is inversely proportional to the temperature). The two processes must be taken into account simultaneously in all orders of perturbation theory and in the more complex diagrams. However, the suppression of the scattering of particles by each other in the case $\nu = \frac{1}{2}$ is still evidence for the excitation of charge density waves at this density. Finding a definitive answer to this question will require a more detailed analysis of the perturbation-theory series. Such an analysis goes beyond the scope of the present paper.

Finally, there is another, extremely important circumstance to be noted. A simultaneous diagonalization of the Cooper and zero-sound loops (Fig. 2) can be carried out by going over to exciton variables.[6] The eigenfunctions are

$$\delta(p_1' - p_1 - k_y) \exp[^{1}/_{2} i k_x (p_1' + p_1)],$$
$$\delta(p_2 - p_2' - k_y) \exp[^{1}/_{2} i k_x (p_2 + p_2')],$$

where the momentum $\mathbf{k} = (k_x, k_y)$ corresponds to the momentum of the exciton (in the case at hand, it corresponds to a charge density wave).

[1] Yu. A. Bychkov, S. V. Iordanskiĭ, and G. M. Éliashberg, Pis'ma Zh. Eksp. Teor. Fiz. **33**, 152 (1981) [JETP Lett. **33**, 143 (1981)].
[2] R. B. Laughlin, Phys. Rev. Lett. **50**, 1395 (1983).
[3] I. V. Lerner and Yu. E. Lozovik, Zh. Eksp. Teor. Fiz. **82**, 1188 (1982) [Sov. Phys. JETP **55**, 691 (1982)].
[4] Yu. A. Bychkov, Fiz. Tverd. Tela (Leningrad) **31**(7), 56 (1989) [Sov. Phys. Solid State **31**(7), 1130 (1989)].
[5] H. Fukuyama, P. M. Platzman, and P. W. Anderson, Phys. Rev. B **19**, 5211 (1979).
[6] Yu. A. Bychkov and É. I. Rashba, Zh. Eksp. Teor. Fiz. **85**, 1826 (1983) [Sov. Phys. JETP **58**, 1062 (1983)].
[7] A. A. Abrikosov, L. P. Gor'kov, and I. E. Dzyaloshinskiĭ, *Quantum Field-Theoretical Methods in Statistical Physics*, Fizmatgiz, Moscow, 1962 (Pergamon, New York, 1965).
[8] A. Z. Patashinskii and V. L. Pokrovskii, *Fluctuation Theory of Phase Transitions*, Nauka, Moscow, 1982, Chap. X (a previous edition of this book has been published in English translation by Pergamon, Oxford, 1979).

Translated by D. Parsons

407   Sov. Phys. JETP **73** (2), August 1991

A. V. Andreev and Yu. A. Bychkov   407